



Sheet sealing in single and multilayer nanopapers

Hamidreza Ahadian¹ · Elaheh Sharifi Zamani · Josphat Phiri · Miguel Alexandre Salvador Coelho · Thaddeus Maloney

Received: 6 April 2022 / Accepted: 2 July 2022 / Published online: 20 July 2022
© The Author(s) 2022

Abstract This study addresses one of the limiting factors for producing micro and nanofibrillated cellulose (MNFC)-containing papers: poor water removal properties. We focus on the sheet sealing phenomenon during dewatering. A modified dynamic drainage analyzer (DDA) is used to examine both multilayer and single layer forming of MNFC and pulp mixtures. It was found that a thin layer of pulp fibers on the exit layer with the grammage as low as 5 gsm was enough to significantly improve the dewatering of MNFC. For example, the dewatering rate of a furnish with 50% MNFC increased from 0.6 mL/s for a mixed system to 2 mL/s for multilayer system. However, the sheet sealing behavior was completely different when a lower proportion of MNFC was used. For the furnishes with less than 20% MNFC content, the mixed furnishes dewatered faster because the high

amount of pulp fibers were able to prevent MNFC from enriching on the exit layer. Surprisingly, we found that very high final solids content (couch solids) could sometimes be achieved when MNFC was used. The highest solids contents achieved were 34 and 29% for the mixed systems. This compares to the 15–20% range typical of standard papermaking furnishes without MNFC. Overall, the results show that contrary to current thinking MNFC containing papers may lead, under some circumstances, to enhanced wire section dewatering.

Keywords Nanocellulose · Dewatering · Multilayer · Barrier properties · Paper making

Supplementary Information The online version contains supplementary material available at <https://doi.org/10.1007/s10570-022-04751-y>.

H. Ahadian (✉) · E. Sharifi Zamani · J. Phiri · T. Maloney (✉)
Department of Bioproducts and Biosystems, School of Chemical Engineering, Aalto University, Espoo, Finland
e-mail: hamidreza.ahadian@aalto.fi

T. Maloney
e-mail: thaddeus.maloney@aalto.fi

M. A. S. Coelho
RAIZ Forest and Paper Research Institute, Eixo, Aveiro, Portugal

Introduction

During the last decade, there has been an increasing interest in nanopapers. Nanopapers are an emerging category of paper that contains a significant quantity of some nanomaterial(s). Nanopapers can have novel functional properties for a range of applications such as energy storage, packaging etc. (Turbak et al. 1983; Hubbe et al. 2017; Phiri et al. 2018). Micro-nano fibrillated cellulose (MNFC) is one of the most important constituents in many nanopapers. MNFC is the fibrillar residue obtained by deaggregation of cellulosic macrofibers. MNFC may have a 10–100 nm width compared to 10–50 μm for the parent fibers. The addition of MNFC to the paper sometimes leads

to improved strength, barrier, optical, and surface properties (Boufi et al. 2017; Fang et al. 2019; Balea et al. 2020; Das et al. 2020; Lourenço et al. 2020). One of the main challenges for wider scale application of MNFC is poor water removal properties. This is due to small size, large surface area and high swelling ability of MNF fibrils (Taipale et al. 2010; Koponen et al. 2015; Rantanen et al. 2015; Sim et al. 2015; Amini et al. 2019; Sjöstrand et al. 2019; Balea et al. 2020).

One of the important structural parameters affecting dewatering in the fourdrinier paper machine is the exit layer. The exit layer is defined as the sheet interface adjacent to the forming wire from which water exits the web. The density and permeability of the exit layer have a huge impact on the dewatering efficiency (Hubbe et al. 2020; Ahadian et al. 2021). In single sided dewatering, the sheet structure is built up layer by layer under turbulent conditions, especially in the early part of dewatering (Niskanen 2008). In this part of dewatering, fines, fillers or added nanoparticles can move relative to fibers and enrich in the exit layer of the sheet; impeding subsequent dewatering (Hubbe 2002; Hubbe and Heitmann 2007; Hubbe et al. 2020). This phenomenon is called sheet sealing and may be related to the density and permeability of the exit layer or the plugging and loss of permeability of the forming wire (Räisänen 1996; Hubbe and Heitmann 2007; Koponen et al. 2015; Sjöstrand et al. 2019; Hubbe et al. 2020). The actual microscopic mechanisms of sheet sealing are not well understood, but the phenomenon is often observed on industrial paper machines – to the great detriment of running speed and production. Fines content and conformability of a furnish are the major determinant of sheet sealing (Hubbe and Heitmann 2007; Hubbe et al. 2020). Conformability corresponds to the fibrils flexibility and ability to pack, form a dense layer, and block the openings (Doo and Kerekes 1982). For furnishes rich in micro and nanoparticles, the potential for sheet sealing and poor dewatering arises (Hubbe and Heitmann 2007; Hubbe et al. 2020). In normal pulp furnishes, some chemical or mechanical measures are taken to reduce the dewatering resistance. For example, before the forming section in a paper machine, cationic and anionic polyelectrolytes are normally added to the furnish to bind the fines to the fiber surfaces, thus preventing plugging of waterways and improving permeability (Cadotte et al.

2007; Xiao et al. 2009; Taipale et al. 2010; Rice et al. 2018). In addition, short, upward hydraulic pulses are applied to partially refluidize the web structure and disrupt sealing (Räisänen et al. 1993; Neun 1994). However, the addition of a significant amount of MNFC can dramatically worsen dewatering, and these conventional measures are not effective in overcoming the dewatering resistance (Turbak et al. 1983; Ahadian et al. 2021).

There have been studies conducted to improve the dewatering of MNFC containing furnishes. Many studies have considered usual wet end parameters such as pH, conductivity and polyelectrolyte type and concentration (Mörseburg and Chinga-Carrasco 2009; Taipale et al. 2010; Korhonen 2015; Maloney 2015; Sim et al. 2015; Merayo et al. 2017; Sjöstrand et al. 2019). For instance, Sim et al. (2015) studied the induced aggregation of MNFC fibrils by absorbing cationic electrolyte (Na^+ or Ca^{2+}). Brockman et al. (2017) employed high charge density cationic polymer (poly-DADMAC) to modify the surface charge of cellulose nanocrystals. Sethi et al. (2018) achieved rapid water drainage by using lactic acid to hydrophobize the surface of MNFC fibrils, which could decrease the densification of the network. Maloney et al. (2015) could control swelling of TEMPO-oxidized NFC by changing the counterion from Na^+ to Ca^{2+} . Application of shear to the furnish during dewatering has also been used to lower the furnish viscosity and improve dewatering (Dimic-Misic et al. 2013a, b). Recently, one study indicated that optimizing the duration and frequency of vacuum pulses could improve the dewatering of MNFC containing furnishes (Korhonen et al. 2019). Electro-assisted dewatering has also shown potential to improve the dewatering of cellulose nanocrystal suspensions (Wetterling et al. 2018).

One way to control the exit layer is by using a multi-layered approach. Layered paper structures can be made in different ways. One technique is using multilayer headboxes that is also referred to as stratified forming. Briefly, stratified forming is the practice of producing a sheet with multiple layers of different furnishes through one single headbox. Different stock layers are brought together within the headbox or in the jet and simultaneously sprayed onto the fabric and dewatered in one forming unit. This technique has a very good potential for producing optimized web structures with associated savings in raw materials

and production costs. Despite its potential, multi-layer forming has met limitations for low grammage products where layer mixing has proven problematic (Puurtinen 2004; Karlsson et al. 2009; Lucisano et al. 2015; Nordström 2016; Nordström and Hermansson 2017). Multi-ply forming is another approach that involves a successive forming process through which the second ply is directly formed onto the previously formed web (Attwood 1980; Puurtinen 2004; Nordström 2016; Nordström and Hermansson 2017). Multilayer structures are distinctly interesting for MNFC containing products, where the surface functional properties of the MNFC can be combined synergistically with the toughness and cost advantages of fiber furnishes.

This study examines the possible production synergies of MNFC-fiber two-layer structures. The hypothesis is that if the first layer i.e., the exit layer, is made from pulp fibers and the second layer from MNFC, then the dewatering resistance in the exit layer will be reduced and sheet sealing prevented. While the study deals with single sided dewatering directly applicable to Fourdrinier forming, the concepts presented here are more widely relevant to gap and hybrid forming technologies.

Materials and methods

Materials

A once-dried, bleached pine softwood Kraft pulp (BSKP) was provided by a Finnish pulp mill. The pulp was unrefined. The pulp sheet was disintegrated in a valley beater according to ISO 6264/1; then, it was stored at 8% wt.

MNFC was provided by Suzano Pulp and Paper at 5%wt solids. The MNFC was produced by mechanical defibrillation of eucalyptus hardwood Kraft pulp. The pulp and MNFC properties are shown in Table 1. The drainability of pulp was measured according to ISO 5267-1:1999. The fiber length and fines content were measured with Fiber Analyzer (Valmet Fiber Image Analyzer FS 5). In this method, the flake-like solids shorter than 0.2 mm is considered as fines, and fines content is determined as a percentage of the projection area of measured particles. The water

Table 1 Properties of pulp and MNFC (* Fraction above 0.2 mm)

Properties	Materials	
	BSKP	MNFC
Drainability ($^{\circ}$ SR)	13.6	–
WRV ($\frac{g_{\text{water}}}{g_{\text{solid}}}$)	1.00	4.49
Length weighted fiber length (mm) *	2.02	0.33 *
Fiber width (μm)	28.0	3.5
Fines content (smaller than 0.2 mm, length weighted average) (%)	10.18	75.96
Viscosity (mPa.s)	–	13,283
Transmittance (%)	–	23.88
Zeta potential (mV)	–20.6	–31.6

retention value (WRV) of the pulp was measured based on SCAN-C 102 XE.

The WRV of MNFC was measured according to the method developed by Maloney (2015). The viscosity was measured with a Brookfield viscometer DV2T-RV at 10 rpm and 1.5%wt using a vane spindle V-72. Transmittance was measured using a UV-Vis spectrophotometer 2550 (Shimadzu, US) at wavelength 800 nm and consistency 0.1%wt (Kangas et al. 2014; Phiri 2019). The zeta potential was measured using a ZetaSizer Nano ZS instrument (Malvern Instruments, UK) at 0.1 wt% consistency. Figure 1 shows the light microscopy image of the MNFC.

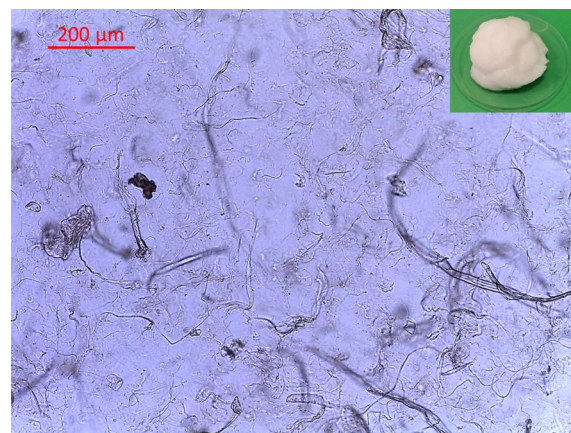


Fig. 1 Light microscopy image of the MNFC

Dewatering experiments

In one series, six furnishes were prepared from MNFC and BSKP. The MNFC grammage was fixed at 20 gsm while BSKP grammages were 5, 10, 20, 40, 60 and 80 gsm, respectively. These experiments were conducted at vacuum pressures of 50 mbar and 700 mbar. In these experiments, the total grammage of furnishes is varied.

In another series, seven furnishes with a constant grammage of 100 gsm but different MNFC and BSKF compositions were also made. The MNFC grammages were 50, 30, 20, 10, 5, 2, 0 gsm and the BSKF grammages were 50, 70, 80, 90, 95, 97, 100 gsm, respectively. The dewatering experiments were conducted at 700 mbar.

To prepare the furnishes, BSKP and MNFC were separately disintegrated in a British L&W disintegrator for 12,000 revolutions. Furnish preparation and measurements were performed at room temperature. Deionized water was used for all experiments.

The dewatering experiments were performed in a modified Dynamic Drainage Analyser (DDA 5, Pulp-Eye, Sweden) with a 10 cm diameter etched screen from nickle with 50 μm conical holes (50W050P10N, Gronmark, Finland). For the dewatering, a certain vacuum pressure was applied for 300s. Vacuum pressure changes were measured throughout the dewatering time. An ultrasonic level sensor on top of the DDA vessel continuously measures the furnish volume during dewatering. A sheet collected after dewatering is used to evaluate the final solids content gravimetrically. The final solids content of the sheets (couch solids) is the mass fraction of oven dried solids in the web after the vacuum period.

Forming approaches

The sheets were formed in two different ways. The first method is a single layer forming of a mixed furnish of BSKP and MNFC. The second way is multilayer forming by first forming a BSKP layer, followed by a second MNFC layer directly formed on top of the pulp layer. All the test points were done with both single layer forming and multilayer forming.

For the single layer mixture forming, the total required amount of BSKP and MNFC were mixed, diluted up to 300 ml, added to the DDA vessel, mixed

at 300 rpm for 10 s, followed by 10 s rest time before dewatering commenced.

For the multilayer forming, each of the BSKP and MNFC were diluted to 300 ml separately. The fiber layer was prepared by forming a BSKP web which was then transferred to a 105 °C oven and dried with a 1 kg weight on top. The idea in this approach is that the initially dry fiber substrate has enough cohesion to withstand the hydrodynamic forces of a MNFC suspension being dewatered through it (Fig. 2part a&b).

To add MNFC suspension, an inner sleeve with a perforated bottom with 1 mm holes goes inside the DDA vessel so that the bottom face positioned 1 cm above the substrate (Fig. 2part c, and Fig. 3). This is used to help distribute the MNFC furnish without disturbing the fiber layer. Then the sleeve is removed, and MNFC layer is formed on top of the fiber layer (Fig. 2part d). The sheet is dried in the oven with a 1 kg weight on top (Fig. 2part e).

Characterization of the sheets

The formed paper samples were dried at 105 °C in the oven with a 1 kg weight on top. This was done to prevent shrinkage especially for the sheets with higher MNFC contents. The dried sheets were conditioned for 48 h before testing at a temperature of 23 °C and relative humidity of 50% according to standard ISO 187:1990.

The air permeability was measured with Gurley-Hill SPS according to the standard SCAN-P 19:78.

The water vapor barrier properties of the sheets were measured with the water vapor transmission testing instrument (Labthink PERME® W3/230) according to ISO 15106-2:2003. The specimen area was 5.31 cm², and the thickness of the film was measured before analysis with a micrometer. The measurements were carried out at 38 °C, normal atmospheric pressure, 90% RH and 100 ml/min gas flow rate.

The oxygen barrier properties were measured with an oxygen permeability tester (Labthink PERME OX2/230) according to ISO 15105-2:2003. The samples were conditioned before testing at the temperature of 23 °C and relative humidity of 0% for at least 24 h. The measurements were carried out at 23 °C, normal atmospheric pressure, 0% RH and 10 ml/min gas flow rate.

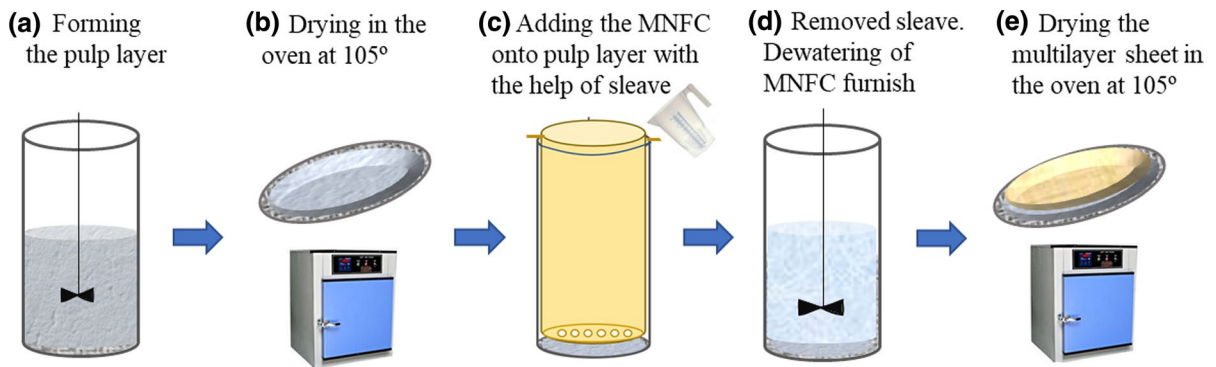


Fig. 2 Schematic of multilayer dewatering experiments

Fig. 3 The cylinder with perforated bottom was used to add MNFC suspension for multilayer forming



Results and discussion

A dewatering experiment in the DDA is an example of a classical one-dimensional filtration method. While this is simplified compared to dewatering phenomena on a paper machine, it can still reflect beneficial information about the industrial dewatering behavior of a furnish (Ahadian et al. 2021). In this study, the material and screen system have been selected to avoid using chemical retention aids that would be absolutely required in practical papermaking conditions.

We compared the dewatering efficiency of a mixture and multilayer system of pulp and MNFC in DDA. Figure 4 shows the dewatering curves of furnishes at two different vacuum levels with constant MNFC and varying BSKP content. As the pulp content increases in the mixed system, the dewatering becomes faster. At less than 40 gsm BSKP contents, the sheet was sealed entirely before dewatering could complete. This can be seen in Fig. 4a and b, where the furnish reaches a quasi-equilibrium state and effectively stops dewatering with much of the water remaining.

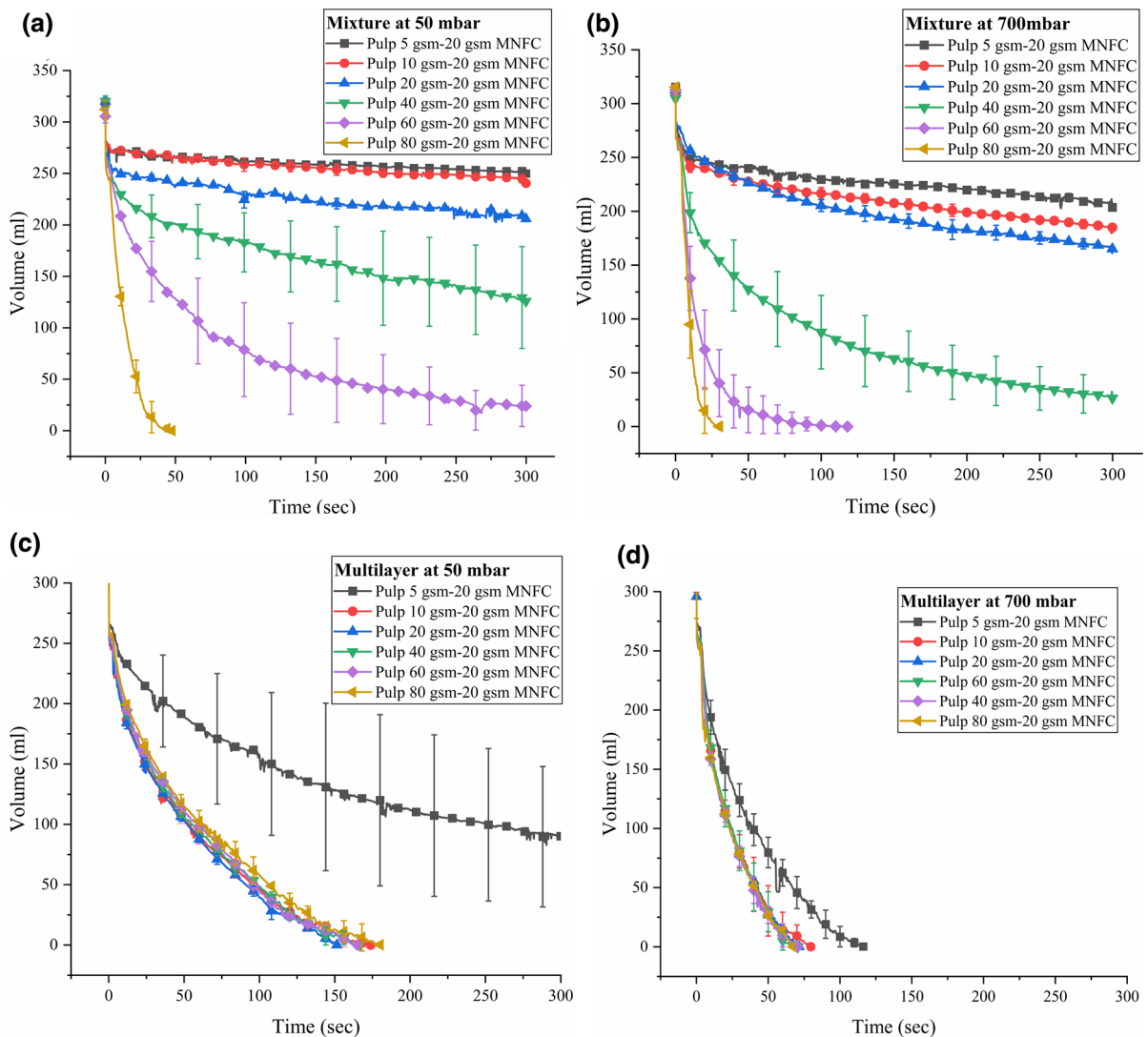


Fig. 4 Furnish volume during dewatering. **a** Mixed furnishes at 50 mbar vacuum **b** Mixed furnishes at 700 mbar vacuum **c** Multilayer furnishes at 50 mbar vacuum **d** Multilayer furnishes at 700 mbar vacuum

The sealed exit layer is visible on the SEM image of sheets with 5 and 20 gsm pulp content (Fig. 5a and c). The image shows that the sealing is due to the enrichment of MNFC at the exit layer. When the MNFC proportion in a furnish decreases, the presence of MNFC on the exit layer also decreases (Fig. 5e), which leads to less clogging of the exit layer and, thus much faster dewatering.

It is interesting to note that between 40 gsm and 60 gsm pulp content, unstable dewatering takes place. For some replicates, the sheet will completely dewater, and for others the sheet will seal,

and dewatering will effectively stop. This transient behavior is due to random and uneven enrichment of MNFC in the exit layer. The dewatering, in this case, is very unpredictable, which can be seen from the high standard deviation in Fig. 4a and b.

Comparing the SEM images of the “fast” and “slow” dewatered samples in the above-mentioned transient behavior gives a better understanding of sheet sealing phenomenon. Figure 6 shows the wire side of samples, what we call the exit layer. In the sample with slow dewatering (Fig. 6a), MNFC appears to enrich around the plate’s discrete conical

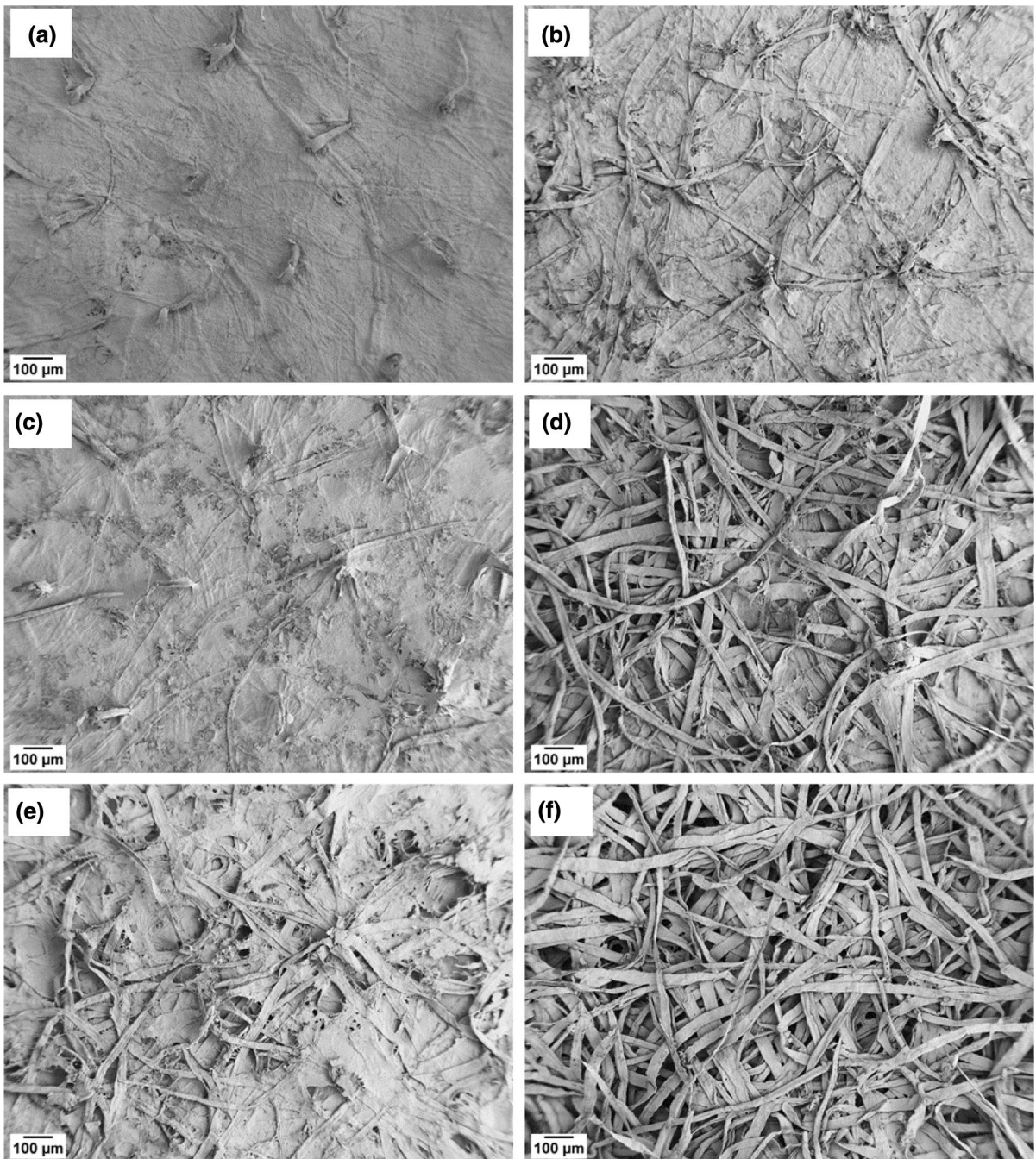


Fig. 5 SEM images of the wire side of the sheets **a** Mixed furnish of Pulp 5gsm-MNFC 20gsm, **b** Multilayer furnish of Pulp 5gsm-MNFC 20gsm, **c** Mixed furnish of Pulp 20gsm-MNFC 20gsm, **d** Multilayer furnish of Pulp 20gsm-MNFC 20gsm,

e Mixed furnish of Pulp 80gsm-MNFC 20gsm, **f** Multilayer furnish of Pulp 80gsm-MNFC 20gsm (The images on the left side belong to mixed sheets and vice versa)

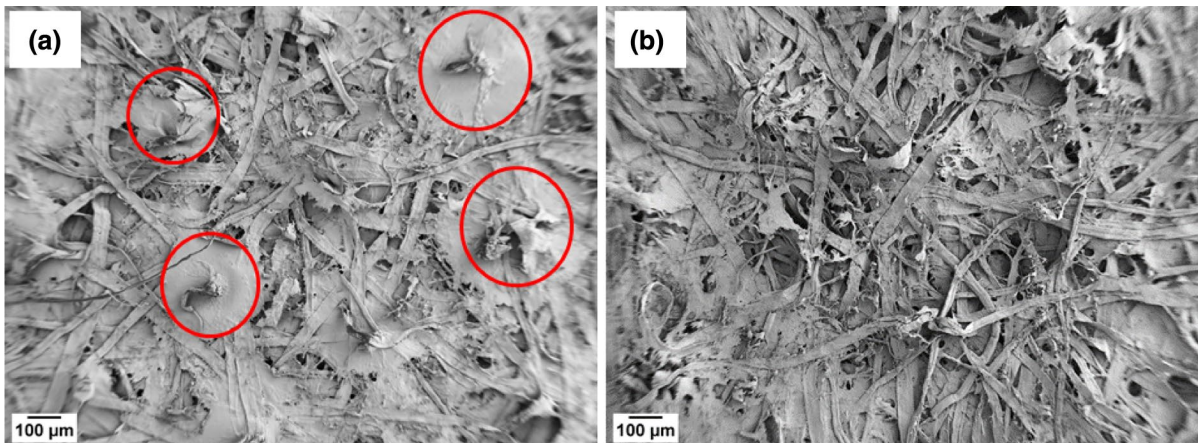


Fig. 6 SEM images of a wire side of the mixed sheets **a** Pulp 60gsm-MNFC 20gsm with slow drainage, **b** Pulp 60gsm-MNFC 20gsm with fast drainage

holes (red circles) and fibers are visibly pulled out of the sheet plane into the plate holes. The combination of MNFC enrichment around the holes and pulled fibers into the holes seals the sheet and hinders dewatering. However, for the fast dewatered sample, the blockage of the holes is not observed, as shown in Fig. 6b.

It is thought that one of the critical mechanisms of sheet sealing on paper machines is the localized plugging of the machine wire (Hubbe et al. 2020). This result gives evidence that the combination of fiber conformation and fines enrichment may be important in sheet sealing. It furthermore suggests that when larger quantities of MNFC is used in paper manufacture, there may be situations where dewatering is in the transient regime, leading to drainage instabilities and runnability issues.

Increasing vacuum from 50 mbar to 700 mbar shifts the transient samples with 60 and 40 gsm fibers toward complete dewatering. The error bars in Fig. 4b for these samples were also reduced, indicating dewatering became more stable. Note that in paper machine dewatering, it is well known that high initial dewatering can seal the sheet and impede dewatering in later stages. In the present study, we have not considered the water removal profile and only examined steady-state dewatering.

The dewatering in a multilayer system is quite different and usually faster than the mixture (Fig. 4c and d). The pulp layer on the screen prevents the sealing of the exit layer. Therefore, the dewatering completes

for the majority of furnishes in less than 170 s, even at 50 mbar vacuum.

To understand why dewatering of a multilayer system is usually faster than a mixed furnish, cross-sectional SEM images of the sheets can help (Fig. 7). A very dense sheet is observed in the mixed system, showing very few channels for water to exit the sheet. However, the overall sheet density is lower for the multilayer system, and the fiber network provides flow channels (Fig. 7-b).

In the multilayer system, the sample with 5 gsm fiber layer has slower dewatering than other samples (Fig. 4). Figure 8 reveals the reason; Light microscopy images of the substrates on the screen show that the 5 gsm fiber layer could not cover the screen thoroughly, and MNFC fibrils still access and clog the holes on the screen. However, the dewatering is still much faster than the dewatering of a similar mixed furnish. In Fig. 5a and b, the SEM image of the exit layer shows much less MNFC enrichment in the multilayer sheet compared to the mixed furnish. This shows that having only a very thin substrate of long fibers (5 gsm) could effectively help dewatering by alleviating the blockage of screen holes.

Interestingly, when the grammage of the pulp increased beyond 5 gsm, MNFC dewatering was not affected by the thickness of the fiber exit layer at neither 50 nor 700 mbar (Fig. 4c and d). This is because, at higher grammages, the fibers cover the entire screen homogeneously and prevent the MNFC fibrils from reaching and clogging the screen. This

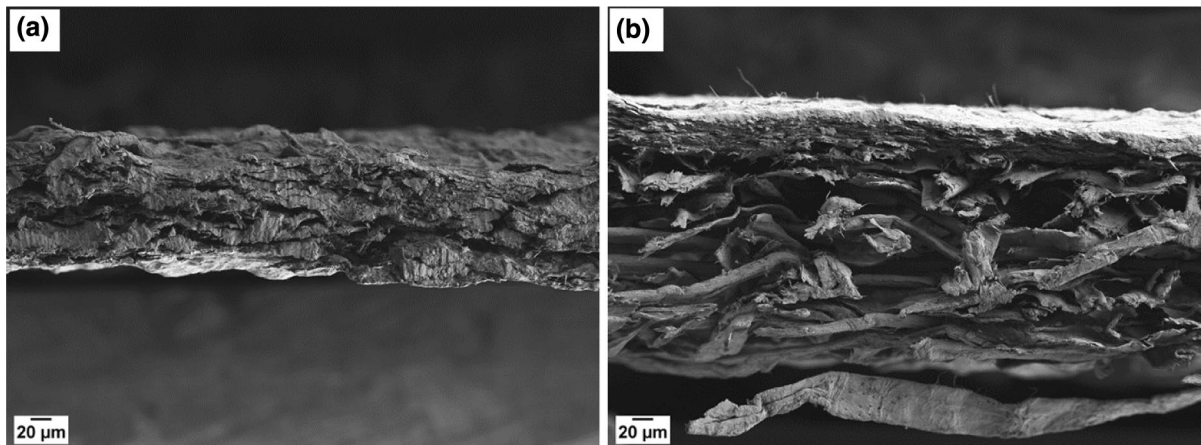
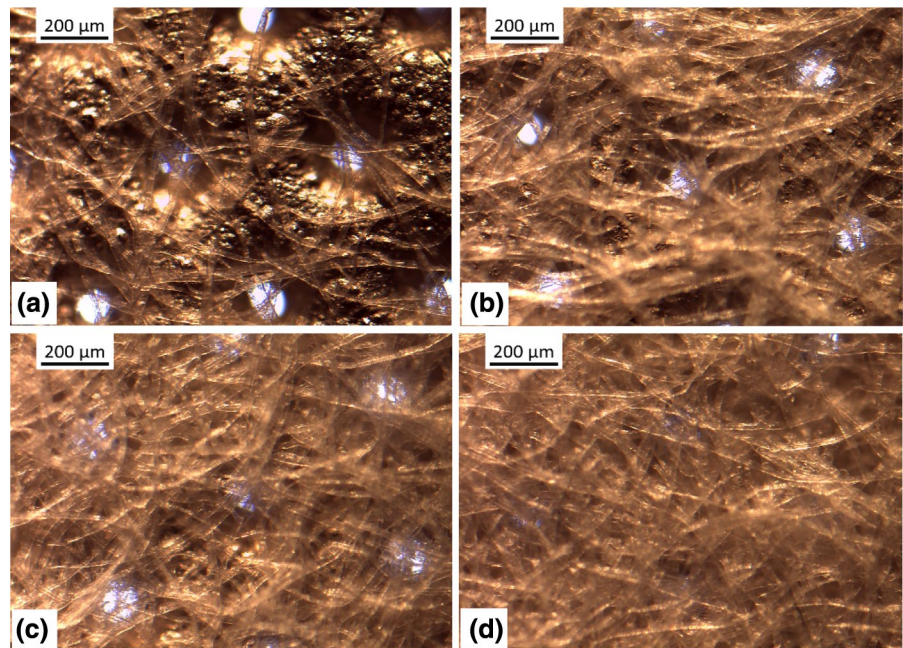


Fig. 7 Cross-sectional SEM images of the sheets, **a** Mixed furnish of Pulp 50gsm-MNFC 50gsm, **b** Multilayer furnish of Pulp 50gsm-MNFC 50gsm

Fig. 8 Light microscopy images of the pulp substrate on top of the metal screen **a** 5 gsm, **b** 10 gsm, **c** 15 gsm, **d** 20 gsm. The rough black texture seen on the image is the metallic surface of the screen



observation is supported by the SEM images in Fig. 5d and f; almost no MNFC can be seen on the wire side of the multilayer sheets with high pulp grammages.

Although the dewatering is generally faster in a multilayer system, the mixed system surpasses the multilayer at 80 gsm pulp content (Fig. 4a and c). This is because, at 80 gsm pulp grammage, the MNFC enrichment on the exit layer probably gets lower than what is needed to seal it completely

(Fig. 5e), simultaneously, the presence of long fibers between MNFC fibrils can disrupt the formation of a dense layer.

Analysis of vacuum level's variations gives further understanding about dewatering (Fig. 9). When free water is being removed from the furnish under steady-state conditions, the vacuum level is constant. The vacuum level starts to decrease when air displaces inter-fiber water and creates air channels through the sheet.

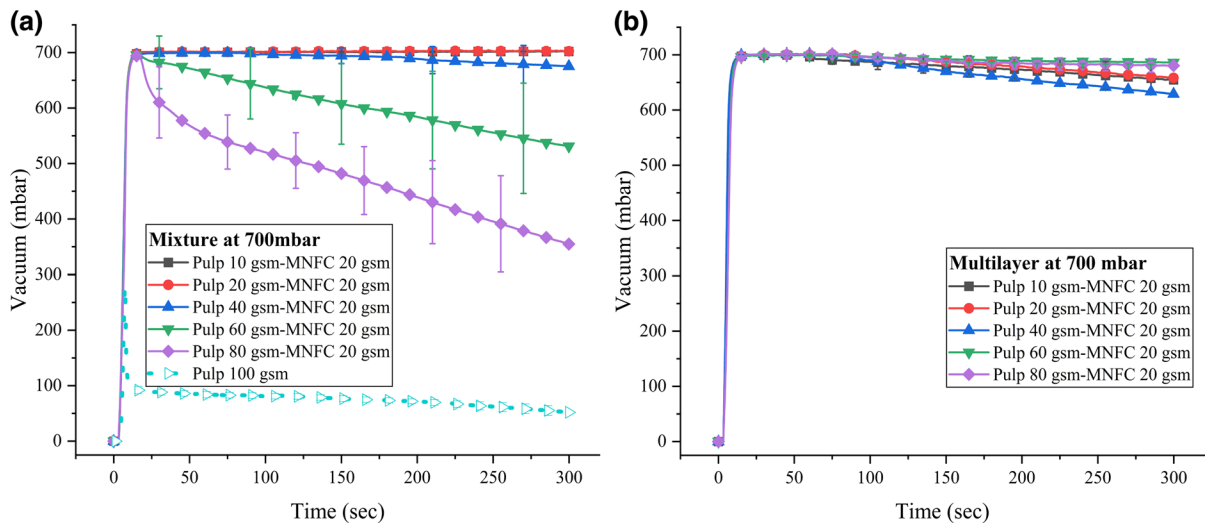


Fig. 9 Vacuum curves as a function of time during dewatering with 700 mbar vacuum of **a** Mixed furnishes, **b** Multilayer furnishes

Table 2 The final solid content of sheets (couch solids) with nominal 20 gsm MNFC dewatered at 50 and 700 mbar; N/A means the dewatering of these furnishes stopped incomplete

Fiber layer grammage (gsm)	Couch solids content (%)			
	50 mbar		700 mbar	
	Mixed	Multilayer	Mixed	Multilayer
10	N/A	7.7 ± 0.3	N/A	14.0 ± 0.5
20	N/A	8.0 ± 0.1	N/A	14.6 ± 0.9
40	N/A	8.9 ± 0.5	N/A	17.3 ± 1.1
60	N/A	10.5 ± 0.3	29.0 ± 2.3	20.7 ± 0.9
80	11.8 ± 0.2	10.8 ± 0.4	34.1 ± 0.6	22.7 ± 0.4

For the majority of the mixed and multilayer samples, the vacuum remains almost constant throughout suction time (Fig. 9). This is because the MNFC decreases sheet permeability, and 700 mbar vacuum is not high enough to overcome surface tension forces and displace water from the interfiber capillaries. For the pure pulp sheet, the vacuum drops quickly and is nearly constant thereafter. The highly permeable sheet does not increase in solids with longer dewatering times. However, for the mixed furnishes with 60 and 80 gsm pulp, the vacuum level decreases monotonically over the entire dewatering event (Fig. 9a). This implies that there is gradual displacement of water by air and an increase in sheet solids over time. This shows how different sheet permeabilities and distributions of

MNFC in the fiber matrix can lead to very different dewatering behavior (Attwood 1962; Räisänen 1996; Åslund and Vomhoff 2008).

The water removal after initial sheet formation can also be examined by considering couch solids after the vacuum period is complete (300s in our experiment). As the pulp grammage increases, the couch solids also increases (Table 2). This is because higher sheet grammage increases sheet compression while under vacuum (Räisänen 1998; Hubbe and Heitmann 2007; Åslund and Vomhoff 2008; Ahadian et al. 2021). Lower WRV of the pulp could also be a reason to achieve higher couch solids. Dewatering was incomplete for the mixed furnishes under 60 gsm pulp grammage; therefore, solids content values are unavailable.

We reached 34 and 29% wt couch solids for the 60 and 80 gsm mixed furnishes at 700 mbar vacuum. This is likely caused by stronger compression and air displacement (Hubbe and Heitmann 2007; Åslund et al. 2008). This is a very high solids compared typical paper machine couch solids, which are usually around 20% solids (Hubbe and Heitmann 2007). We have also observed this behavior in earlier nanopaper pilot trials (Rantanen et al. 2015). It appears that for some nanopaper furnishes very high prepress solids contents are feasible, possibly leading to low energy and other favorable manufacturing considerations. It is necessary to mention that the MNFC retention was not a big issue in these experiments, and more than

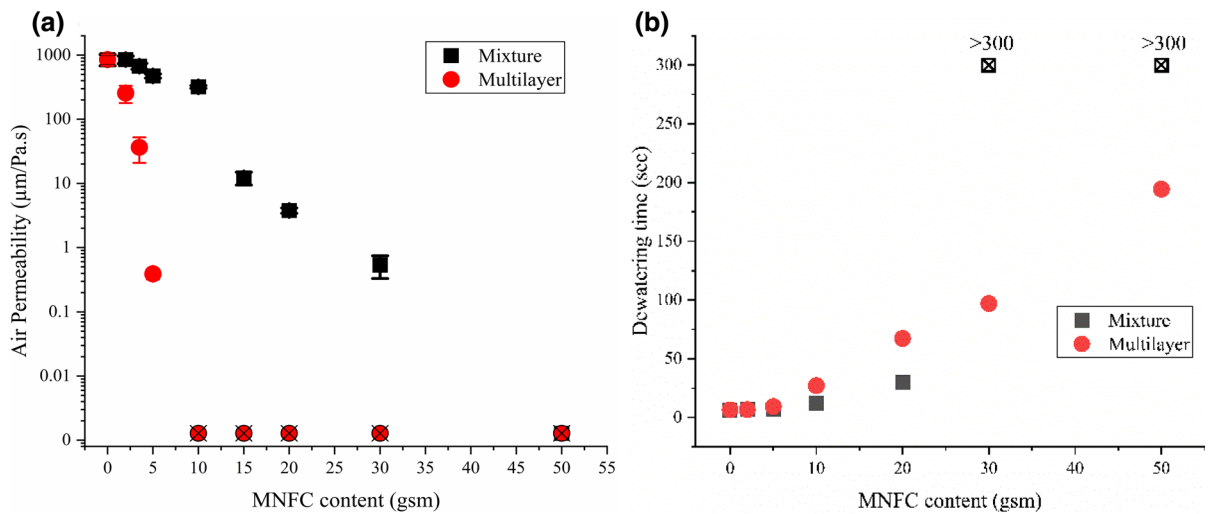


Fig. 10 Properties of 100 gsm mixed and multilayer sheets at different MNFC contents **a** Air permeability of the **b** Dewatering time, (the cross × on some of the air permeability data indicates these were below device resolution)

Table 3 Barrier properties of 100 gsm multilayer sheets; OTR: oxygen transmission rate; OPC: oxygen permeability coefficient; WVTR: water vapor transmission rate; WVPC:

water vapor permeability coefficient; *: the value exceeded the measuring range of the used instrument which is 61,000 cm³/m².d for OTR and 700 g/m² d for WVTR

Pulp (gsm)	MNFC (gsm)	OTR (cm ³ /m ² .d)	OPC (cm ³ .µm/m ² .d.kPa)	WVTR (g/m ² d)	WVPC (g µm/m ² .d.kPa)
98	2	*	*	*	*
95	5	*	*	648.7	33,370
90	10	5726	19,530	671.4	37,410
80	20	23	71	655.9	32,880

85% of the MNFC could retain in each sheet. The actual grammage of each sheet has been reported in supplementary results.

One of the important targets of the fiber-based packaging industry is to produce paper and board grades with barrier properties that meet or exceed those from plastic. In particular, oxygen and water barrier properties are critical in many food packaging products. In this paper, we have demonstrated that the enrichment of MNFC to the top layer of a multilayer web can lead to significantly improved dewatering properties under some conditions. It is interesting to consider whether this concept can also be used to generate improved barrier properties. For this reason, we produced new sheets in which the total grammage is constant, but the pulp to MNFC ratio changes.

In Fig. 10, the air permeability and dewatering time for the mixed and multilayer structures is

shown as a function of MNFC content. The multilayer structure has much lower permeability over the whole range of MNFC content (Fig. 10a). Notably, very low permeability can be achieved at a 10 gsm MNFC layer. In this range, dewatering is still very good for the multilayer web (Fig. 10b). There might be some differences between the air permeability of the multilayer sheets with 10 gsm MNFC layer and more which are below the device's resolution.

The oxygen and water vapor permeability for some of the sheets were measured and reported in Table 3. Between 10 and 20 gsm MNFC, the oxygen permeability drops to a low value, indicating a largely nonporous structure is achieved in that range. Water permeability does not reduce below a threshold value because water is able to absorb into the cellulosic material and diffuse through the solid structure. Water vapor barrier, or oxygen barrier at

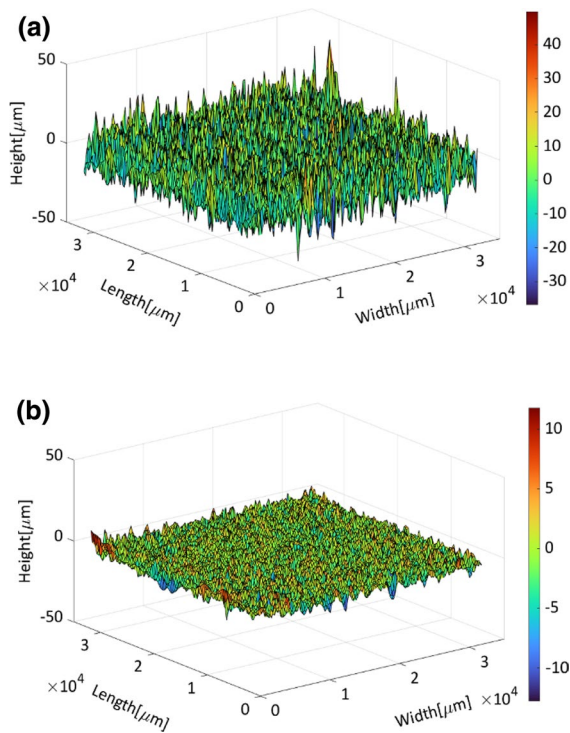


Fig. 11 Topography of top side the 3.5 × 3.5 cm sample Pulp 80gsm-MNFC 20gsm **a** Mixed sheet, **b** Multilayer sheet

high RH, will require further engineering steps such as hydrophobization and/or additional layers.

As part of a multilayer packaging solution, the fiber/MNFC structure also has the advantage that the MNFC layer is relatively smooth. This is shown in Fig. 11. A smooth surface is desirable as a base for a topcoat to add a printing surface or to enhance barrier properties. Smooth substrates are ideal for thin layers of fine particle coatings – perfect for achieving high performance at low material cost.

Conclusions

Sheet sealing is one of the main challenges of using nanocellulose in nanopapers. Finding a way to mitigate this problem could open new ways of producing functional nanopapers with high MNFC content. In this study, we proposed multilayer forming approach to overcome sheet sealing issue. By first forming a layer of long fibers on the sheet, this could prevent the nanocellulose from reaching and clogging the exit

layer. It was shown that the pulp grammage as low as 5 gsm is enough to prevent sheet sealing and it was possible to dewater a furnish with as high as 50% of MNFC. Once the whole sheet surface is covered by the fibers, further increase in substrate thickness does not affect dewatering. The interface between fibers and the MNFC layer act as the exit layer for the MNFC furnish. In some cases, homogenous mixtures of the MNFC give better dewatering than multilayer structures. The MNFC/fiber mixture maintains a permeable structure throughout the dewatering event and can lead to very high couch solids. Under some conditions MNFC/fiber multilayer forming may be useful to produce paper board with enhanced barrier properties. Multilayer forming has the potential for the fabrication of functional nanopapers for a range of applications such as packaging.

Acknowledgments This research was funded by Jane and Aatos Erkko foundation. This work made use of Aalto University Bioeconomy Facilities. The SEM imaging was conducted at Aalto University Nanomicroscopy Centre (Aalto-NMC). The authors appreciate support from RAIZ Forest and Paper Research Institute and the Impactus project for conducting barrier properties measurements.

Author contributions HA has done the main job of this study. Other authors had sufficient contribution to the concept design, material preparation, data collection, data analysis and writing. All authors read, revised, and approved the final manuscript.

Funding Open Access funding provided by Aalto University. This work was supported by Jane and Aatos Erkko foundation (3269-7422e).

Declarations

Conflict of interest The authors report no conflicts of interest. The authors alone are responsible for the content and writing of the paper.

Open Access This article is licensed under a Creative Commons Attribution 4.0 International License, which permits use, sharing, adaptation, distribution and reproduction in any medium or format, as long as you give appropriate credit to the original author(s) and the source, provide a link to the Creative Commons licence, and indicate if changes were made. The images or other third party material in this article are included in the article's Creative Commons licence, unless indicated otherwise in a credit line to the material. If material is not included in the article's Creative Commons licence and your intended use is not permitted by statutory regulation or exceeds the permitted use, you will need to obtain permission directly from the copyright holder. To view a copy of this licence, visit <http://creativecommons.org/licenses/by/4.0/>.

References

- Ahadian H, Sharifi Zamani E, Phiri J, Maloney T (2021) Fast dewatering of high nanocellulose content papers with in-situ generated cationic micro-nano bubbles. Dry Technol. <https://doi.org/10.1080/07373937.2021.1942898>
- Amini E, Tajvidi M, Bousfield DW et al (2019) Dewatering behavior of a wood-cellulose nanofibril particulate system. Sci Rep 9:1–10. <https://doi.org/10.1038/s41598-019-51177-x>
- Åslund P, Vomhoff H (2008) Dewatering mechanisms and their influence on suction box dewatering processes – A literature review. Nord Pulp Pap Res J 23:389
- Åslund P, Vomhoff H, Waljanson A (2008) The deformation of chemical and mechanical pulp webs during suction box dewatering. Nord Pulp Pap Res J 23:403
- Attwood BW (1962) A study of vacuum box operation. Pap Technol 3:446–455
- Attwood BW (1980) Multi-ply web forming-past, present, and future
- Balea A, Fuente E, Concepcion Monte M et al (2020) Industrial application of nanocelluloses in papermaking: a review of challenges, technical solutions, and market perspectives. Molecules 25:526
- Boufi S, González I, Delgado-Aguilar M, et al (2017) Nanofibrillated cellulose as an additive in papermaking process. In: Cellulose-reinforced nanofibre composites: production, properties and applications. pp 153–173
- Brockman AC, Hubbe MA (2017) Charge reversal system with cationized cellulose nanocrystals to promote dewatering of a cellulosic fiber suspension. Cellulose 24:4821–4830. <https://doi.org/10.1007/s10570-017-1477-5>
- Cadotte M, Tellier ME, Blanco A et al (2007) Flocculation, retention and drainage in papermaking: A comparative study of polymeric additives. Can J Chem Eng 85:240–248. <https://doi.org/10.1002/cjce.5450850213>
- Das AK, Islam MN, Ashaduzzaman M, Nazhad MM (2020) Nanocellulose: its applications, consequences and challenges in papermaking. J Packag Technol Res. <https://doi.org/10.1007/s41783-020-00097-7>
- Dimic-Misic K, Puisto A, Gane P et al (2013a) The role of MFC/NFC swelling in the rheological behavior and dewatering of high consistency furnishes. Cellulose 20:2847–2861
- Dimic-Misic K, Puisto A, Paltakari J et al (2013b) The influence of shear on the dewatering of high consistency nanofibrillated cellulose furnishes. Cellulose 20:1853–1864. <https://doi.org/10.1007/s10570-013-9964-9>
- Doo PAT, Kerekes RJ (1982) The flexibility of wet pulp fibres. Pulp Pap Canada 83:46–50
- Fang Z, Hou G, Chen C, Hu L (2019) Nanocellulose-based films and their emerging applications. Curr Opin Solid State Mater Sci 23:100764
- Hubbe MA (2002) Fines management for increased paper machine productivity. In: Proc Sci Tech Advan Wet End Chemistry. pp 1–22
- Hubbe MA, Heitmann JA (2007) Review of factors affecting the release of water from cellulosic fibers during paper manufacture. BioResources 2:500–533. <https://doi.org/10.15376/biores.2.3.500-533>
- Hubbe MA, Ferrer A, Tyagi P et al (2017) Nanocellulose in thin films, coatings, and plies for packaging applications: a review. BioResources 12:2143–2233
- Hubbe M, Sjöstrand B, Nilsson L et al (2020) Rate-limiting mechanisms of water removal during the formation, vacuum dewatering, and wet-pressing of paper webs. Rev BioResources 15:9672–9755
- Kangas H, Lahtinen P, Sneek A et al (2014) Characterization of fibrillated celluloses. A short review and evaluation of characteristics with a combination of methods. Nord Pulp Pap Res J 29:129–143. <https://doi.org/10.3183/npprj-2014-29-01-p129-143>
- Karlsson H, Beghelli L, Nilsson L, Stolpe L (2009) Handsheet former for the production of stratified sheets. Appita J 62:272–278
- Koponen A, Haavisto S, Liukkonen J, Salmela J (2015) Analysis of the effects of pressure profile, furnish, and microfibrillated cellulose on the dewatering of papermaking furnishes. Tappi J 14:325–337. <https://doi.org/10.32964/tj.14.5.325>
- Korhonen M (2015) Flocculation/deflocculation of cellulosic materials and miner particles by polyelectrolyte complexes and nanocelluloses
- Korhonen M, Puisto A, Alava M, Maloney T (2019) The effect of pressure pulsing on the mechanical dewatering of nanofiber suspensions. arXiv 115267
- Lourenço AF, Gamelas JAF, Sarmento P, Ferreira PJT (2020) A comprehensive study on nanocelluloses in papermaking: the influence of common additives on filler retention and paper strength. Cellulose. <https://doi.org/10.1007/s10570-020-03105-w>
- Lucisano M, Söderberg D, Vomhoff H et al (2015) Stratified forming as a tool for resource efficient papermaking. In: Paper conference and trade show, PaperCon. pp 767–785
- Maloney TC (2015) Network swelling of TEMPO-oxidized nanocellulose. Holzforschung 69:207–213. <https://doi.org/10.1515/hf-2014-0013>
- Merayo N, Balea A, de la Fuente E et al (2017) Synergies between cellulose nanofibers and retention additives to improve recycled paper properties and the drainage process. Cellulose 24:2987–3000. <https://doi.org/10.1007/s10570-017-1302-1>
- Mörseburg K, Chinga-Carrasco G (2009) Assessing the combined benefits of clay and nanofibrillated cellulose in layered TMP-based sheets. Cellulose 16:795–806. <https://doi.org/10.1007/s10570-009-9290-4>
- Neun JA (1994) Performance of high vacuum dewatering elements in the forming section. Tappi J 77:133–138
- Nordström B (2016) Multi-ply forming of linerboard by successive twin-wire roll forming. Nord Pulp Pap Res J 31:613–623. <https://doi.org/10.3183/npprj-2016-31-04-p613-623>
- Nordström B, Hermansson L (2017) Successive twin-wire roll forming of two-ply paper with softwood kraft pulp and recycled pulp - Effect of kraftply formation on Z-strength. Nord Pulp Pap Res J 32:639–645. <https://doi.org/10.3183/NPPRJ-2017-32-04-p639-646>
- Phiri J (2019) Functional properties of mechanically exfoliated graphene

- Phiri J, Johansson LS, Gane P, Maloney TC (2018) Co-exfoliation and fabrication of graphene based microfibrillated cellulose composites-mechanical and thermal stability and functional conductive properties. *Nanoscale*. <https://doi.org/10.1039/c8nr02052c>
- Puurtinen A (2004) Multilayering of fine paper with 3-layer headbox and roll and blade gap former. Helsinki University of Technology, Espoo
- Räsänen K (1996) High-vacuum dewatering on a paper machine wire section: a literature review. *Pap ja puu* 78:113–120
- Räsänen K (1998) Water removal by flat boxes and a couch roll on a paper machine wire section, Doctoral d. Helsinki University of Technology, Helsinki
- Räsänen KO, Paulapuro H, Kärtilä S (1993) Wire section simulation with the moving belt drainage tester (MBDT). In: *PapermakersConference*. Tappi press. <https://doi.org/10.15376/biores.10.2.3492-3506>
- Rantanen J, Dimic-Misic K, Pirttiniemi J et al (2015) Forming and dewatering of a microfibrillated cellulose composite paper. *BioResources* 10:3492–3506. <https://doi.org/10.15376/biores.10.2.3492-3506>
- Rice MC, Pal L, Gonzalez R, Hubbe MA (2018) Wet-end addition of nanofibrillated cellulose pretreated with cationic starch to achieve paper strength with less refining and higher bulk. *Tappi J* 17:395–403. <https://doi.org/10.32964/tj17.07.395>
- Sethi J, Oksman K, Illikainen M, Sirviö JA (2018) Sonication-assisted surface modification method to expedite the water removal from cellulose nanofibers for use in nanopapers and paper making. *Carbohydr Polym* 197:92–99. <https://doi.org/10.1016/j.carbpol.2018.05.072>
- Sim K, Lee J, Lee H, Youn HJ (2015) Flocculation behavior of cellulose nanofibrils under different salt conditions and its impact on network strength and dewatering ability. *Cellulose* 22:3689–3700. <https://doi.org/10.1007/s10570-015-0784-y>
- Sjöstrand B, Barbier C, Ulkten H, Nilsson L (2019) Dewatering of softwood kraft pulp with additives of microfibrillated cellulose and dialcohol cellulose. *BioResources* 14:6370–6383. <https://doi.org/10.15376/biores.14.3.6370-6383>
- Taipale T, Österberg M, Nykänen A et al (2010) Effect of microfibrillated cellulose and fines on the drainage of kraft pulp suspension and paper strength. *Cellulose* 17:1005–1020. <https://doi.org/10.1007/s10570-010-9431-9>
- Turbak AF, Snyder FW, Sandberg KR (1983) Microfibrillated cellulose, a new cellulose product: properties, uses, and commercial potential. In: *J Appl Polym Sci, Appl Polym Symp ITT Rayonier Inc., Shelton, WA*, pp 815–827
- Wetterling J, Sahlin K, Mattsson T et al (2018) Electroosmotic dewatering of cellulose nanocrystals. *Cellulose* 25:2321–2329. <https://doi.org/10.1007/s10570-018-1733-3>
- Xiao L, Salmi J, Laine J, Stenius P (2009) The effects of polyelectrolyte complexes on dewatering of cellulose suspension. *Nord Pulp Pap Res J* 24:148–157. <https://doi.org/10.3183/npprj-2009-24-02-p148-157>
- Niskanen K (ed) (2008) *Paper physics*. Finnish Paper Engineering Association/Paperi ja Puu Oy, Helsinki

Publisher's Note Springer Nature remains neutral with regard to jurisdictional claims in published maps and institutional affiliations.